Nonlinear Dyn (2015) 82:185–199
DOI 10.1007/s11071-015-2148-4

ORIGINAL PAPER

Synchronization of fractional-order chaotic systems using unidirectional adaptive full-state linear error feedback coupling

Andrew Y. T. Leung · Xian-Feng Li · Yan-Dong Chu · Xiao-Bo Rao

Received: 2 November 2014 / Accepted: 7 May 2015 / Published online: 22 May 2015

Abstract Based on the stability theory of fractional-order system, a novel unidirectional adaptive full-state linear error feedback coupling scheme is extended to control and synchronize all of fractional-order differential (FOD) chaotic systems with in-commensurate (and commensurate) orders. The feedback strength is adaptive to an updated law rather than prescribed as a constant. The convergence speed of feedback strength is regulated by a constant. With rigorous linear algebraic theorems and precisely numerical matrix computations, a reasonable interval in which the ultimate final control strength dwells is suggested, and the reliability of synchronization state is guaranteed. It demonstrates that the unidirectional full-state linear feedback coupling scheme can be adopted to control and synchronize FOD chaotic systems directly. Numerical simulations of three representative FOD chaotic systems illustrate the effectiveness of the proposed scheme.

Keywords Fractional derivative · Chaos synchronization · Adaptive law · Full-state linear error feedback · Coupling

A. Y. T. Leung (✉) · X.-F. Li
Department of Architecture and Civil Engineering, City University of Hong Kong, Kowloon, Hong Kong
e-mail: andrewytleung@163.com

Y.-D. Chu · X.-B. Rao
Department of Mathematics, Lanzhou Jiaotong University, Lanzhou, China

1 Introduction

Chaotic behavior had been observed in many natural systems. The most significant property for a deterministic chaotic system is sensitivity to initial conditions. Any arbitrarily small perturbation on the current trajectory may lead to very big differences in future. In the past several decades, chaos control and synchronization have been widely investigated because of imperative needs on the suppression and migration of chaotic motions. Many effective control and synchronization methods have been proposed since several pioneering studies [1–3]. The synchronization of chaos has great potential applications in many disciplines, especially in some areas closely related to our real life, e.g., secret communication [4], neural dynamics [5], mechanical engineering [6], and image encryption [7]. The essence of chaos synchronization is that two chaotic systems follow the same trajectory on the phase space. In the initial state, the drive system may be very different with the response system. Their state functions may be identical but start from different initial conditions [8], are very different in phase space [9], have different orders [10], and have uncertain or mismatching parameters [11–13], and even are disturbed by external inputs [9,11,12]. However, in the synchronization regime, the drive system drives the response system via the transmitted signals rendering the errors in variables of them are stable locally or globally.

Fractional derivatives have a long history over than 300 years, but which are widely used in modeling

realistic systems only recently. Fractional derivatives are able to model memory and hereditary effects observed in physics due to their non-local essence. From the end of last century, it has been observed that nonlinear fractional-order derivatives can also exhibit chaotic motions (see [14–20] and references therein). Controlling and synchronizing the complex behavior in fractional-order differential (FOD) systems using different control schemes recently have been the focus of much attention [15–20]. And it also has great applications in real life [17–20]. Most of synchronization schemes available for integer-order chaotic systems have been verified to be effective in synchronizing FOD chaotic systems [15–20]. However, some schemes are too complex to be applied in practice due to strong nonlinearity themselves may rendering inexpediency or non-robustness. It is precisely because so many uncertainties and intrinsic nonlinearities, eliminating or weakening the nonlinear terms in error dynamical systems is essential. In some more extreme cases, another control scheme has to be involved to eliminate all of the nonlinear terms and readjust the structure of constant matrix [21]. Due to the simple configuration and easy implementation, the unidirectional and bidirectional linear error feedback coupling schemes were adopted to control and synchronize chaotic and hyper-chaotic systems [22–27]. To be more effective, combining linear error feedback coupling scheme with adaptive control [28,29] and active control [30,31] was proposed and applied to both integer-order and FOD chaotic systems. The success of linear state feedback relies on a proper choice of feedback gains. Wu et al. [22] proposed some sufficient synchronization criteria for generalized Lorenz systems via linear state error feedback control. Jiang and Tang [23,24] proposed a generic criterion of global chaos synchronization between two coupled chaotic systems from unidirectional linear error feedback coupling. Li and Liao [25] derived several sufficient conditions for guaranteeing the existence of anti-synchronization in a class of coupled identical chaotic systems via linear feedback control and adaptive linear feedback control. From rigorously mathematical theory, some sufficient conditions of global synchronization for linearly coupled chaotic systems are presented in Lü's paper [26]. However, most of their works have a common problem, that is, the chaotic systems they considered must be able to be decomposed into their linear and nonlinear parts independently [21–25,27,32]. Specifically, the n-dimensional chaotic systems must be able to be rewritten in the form of

$$D^{\alpha}x = F(x) = A_a x + f(x), \tag{1}$$

where $D^{\alpha}x$ refers to a more general derivative of n-dimensional vector x. A_a is a $n \times n$ matrix containing all of the parameters, thereupon $f(x)$ is an $n \times 1$ nonlinear vector function without any parameters.

Indeed, there are a lot of integer-order and FOD chaotic systems that can be represented in the form of (1), such as Chua system [33], Lorenz system [34,35], Chen system [35,36], Lü system [36,37], and the unified system [38]. However, the simplest Rössler system cannot because parameter b is independent of any variables in the third equation. Luckily, the error dynamical system of two linearly coupling Rössler systems can be represented by (1) [24]. Besides Rössler system, many chaotic systems cannot be written as (1) because some parameters are the coefficient of nonlinear terms, e.g., other Lorenz-like systems with integer order or fractional order [39–44]. In order to compensate for such a limitation, in some works, some untamed parameters have to be included in $f(x)$, which is rewritten as $f(x, a)$. Such a unavoidable treatment makes the identification of uncertain parameters impossible if there are. In order to seek the unidirectional linear feedback coupling strengths, $f(x, a)$ or $f(x)$ should be immersed in mathematical constraints. Hereby, the assumption of Lipschitz condition of the functions and the computation of bounded norms of the attractors in Euclidean space are two common approaches. However, it is very hard to work out the local Lipschitz constant for every nonlinear equations in practice [27]. The bounded norms are always evaluated with the boundaries of orbits in phase space [23–25,45]. As a result, these loose approaches always trigger improper outcomes. For instance, the coupling strengths may be very big or unequal. It may bring out unexpected dynamical behavior in experience, such as desynchronization bursts [46] in both one-way and full-state linear couplings [46–49]. Such a desynchronization burst is usually overlooked or difficult to be found because it always starts at a long synchronization time [46]. Better yet, Wang and Liu [50] presented a new scheme for seeking the proper identical control gain by calculating the largest Lyapunov exponent of a chaotic system. This method is very general and splendid because it is based on the average rate of separation of

infinitesimally close trajectories. It informs us that, with very small control strengths (in amplitude), the synchronization of two identical systems can be achieved via full-state linear feedback coupling. This is because the largest Lyapunov exponents of most chaotic systems usually are very small. It was also extended successfully to FOD chaotic Liu system by Wang et al. [42]. Based on the invariance principle of differential equations, Huang [51] proposed a simple adaptive linear feedback scheme to synchronize chaotic systems. Different with the usual linear feedback, the variable feedback strength is automatically adapted to completely synchronize two linear coupling chaotic systems. In an augment system, the feedback coupling terms are linearly dependent on the errors in variables. Although this scheme is very analytical and has been extended extensively [52–57], how to choose a proper regulation factor in the update law should be further investigated because it affects the convergence rate and the final strength of control gains.

Motivated by these considerations, we extend the adaptive full-state linear error feedback coupling scheme to synchronize all of FOD chaotic systems with incommensurate (or commensurate) orders. Based on the stability theory of fractional-order system, the interaction terms are designed with linear error feedback in full state. The feedback strength is not prescribed as a constant, but adaptive to an updated law, which is of integer-order derivative. Following the principles of adaptive full-state linear feedback scheme, the convergence speed of feedback strength is regulated by a constant. A reasonable interval in which the ultimate control strength dwells is suggested. From basic linear algebraic results, it rectifies a previous conclusion that the control gains in the linear coupling feedback strengths should be lower than a critical value [23–25,45]. However, such a critical value is taken as the lower bound of the present adaptive law. The reliability of the control scheme is guaranteed with rigorous linear algebraic theorems and precisely numerical matrix computations. It shows that the unidirectional adaptive full-state linear feedback coupling scheme can be applied on the control and the identical synchronization of FOD chaotic systems without any hesitation. Not matter whether the FOD chaotic systems can be decomposed as (1) or not. Numerical simulations demonstrate the feasibility of adaptive full-state linear feedback control scheme working well on controlling and synchronizing all of FOD chaotic systems with in-commensurate (or commensurate) orders. The cost on stabilizing and achieving identical synchronization of FOD chaotic systems is also very low as long as the regulation factor in the adaptive law is opportune. In addition, the effects of the regulation factors affect the convergence speed, and the final strength is studied dynamically with concrete examples. The present scheme is so simple that it can be realized in physics easily.

2 Prerequisites and mathematical description

2.1 The definition of fractional derivatives

Fractional calculus is a generalization of integration and differentiation to non-integer-order fundamental operator ${}_aD_t^\alpha$, where a and t are the bounds of the operation and $\alpha \in \mathbb{R}$. The continuous FOD operator is defined as [17]

$$ {}_aD_t^\alpha = \begin{cases} \frac{\mathrm{d}^\alpha}{\mathrm{d}t^\alpha} & \alpha > 0, \\ 1 & \alpha = 0, \\ \int_a^t (\mathrm{d}\tau)^{-\alpha} & \alpha < 0, \end{cases} \tag{2} $$

There are a lot of different definitions for FOD [58]. Two frequently used definitions are introduced here to describe αth-order fractional derivative of a function $f(x)$. The first one is named as Riemann–Liouville (R–L) definition. It is the simplest definition about αth-order fractional derivative of a function $f(x)$ with respect to t and the terminal value 0. It is described as [58]

$$ \frac{\mathrm{d}^\alpha f(x)}{\mathrm{d}t^\alpha} = \frac{1}{\Gamma(m-\alpha)} \frac{\mathrm{d}^m}{\mathrm{d}t^\alpha} \int_0^t (t-\tau)^{m-\alpha-1} f(\tau)\mathrm{d}\tau, \tag{3} $$

where m is the first integer larger than α, $m-1 < \alpha \leq m$. $\Gamma(\cdot)$ is the Gamma function,

$$ \Gamma(x) = \int_0^\infty t^{x-1} e^{-t}\,\mathrm{d}t. $$

Note that the term terminal value refers to the lower limit in (3). It may be a nonzero value in the general definition of the FOD. In addition, the Laplace transform is a powerful integral transform, which is used to switch a function from the time domain to the s-domain. The Laplace transform can be used in some cases to solve linear differential equations with given initial conditions. The Laplace transform of the R–L derivative is described as [59]

$$\mathscr{L}\left\{\frac{\mathrm{d}^{\alpha} f(t)}{\mathrm{d}t^{\alpha}}\right\} = s^{\alpha}\mathscr{L}\{f(t)\} - \sum_{k=0}^{m-1} s^{k}\frac{\mathrm{d}^{\alpha-k-1} f(0)}{\mathrm{d}t^{\alpha-k-1}}, \quad m-1 < \alpha \le m. \tag{4}$$

The R–L fractional derivative is not suitable to be treated by the Laplace transform technique because it requires the non-integer-order derivatives of the function $f(t)$ at initial time. Another fractional derivative is named as Caputo definition, which is sometimes called smooth fractional derivative. It is described as [58]

$$\frac{\mathrm{d}^{\alpha} f(x)}{\mathrm{d}t^{\alpha}} = \begin{cases} \frac{1}{\Gamma(m-\alpha)}\int_0^t \frac{f^{(m)}(\tau)}{(t-\tau)^{\alpha+1-m}}\mathrm{d}\tau, & m-1 < \alpha < m, \\ \frac{\mathrm{d}^m}{\mathrm{d}t^m} f(t), & \alpha = m, \end{cases} \tag{5}$$

where m is the first integer larger than α, i.e., $m-1 < \alpha \le m$.

In contrast, the Caputo definition of the fractional derivative is suitable to be treated by the Laplace transform technique. The Laplace transform of the Caputo fractional derivative is [60]

$$\mathscr{L}\left\{\frac{\mathrm{d}^{\alpha} f(t)}{\mathrm{d}t^{\alpha}}\right\} = s^{\alpha}\mathscr{L}\{f(t)\} - \sum_{k=0}^{m-1} s^{\alpha-k-1} f^{(k)}(0), \quad m-1 < \alpha \le m. \tag{6}$$

Contrary to the Laplace transform of the R–L fractional derivative, only integer-order derivatives of function $f(t)$ appear in the Laplace transform of the Caputo fractional derivative [61]. Especially with zero initial conditions, the Laplace transform of the Caputo fractional derivative can be reduced as [60]

$$\mathscr{L}\left\{\frac{\mathrm{d}^{\alpha} f(t)}{\mathrm{d}t^{\alpha}}\right\} = s^{\alpha}\mathscr{L}\{f(t)\}, \quad m-1 < \alpha \le m. \tag{7}$$

In the following studies, Caputo's fractional derivative is used throughout.

2.2 Stability theorems of fractional derivatives

The first theorem is proposed for stability discrimination of in-commensurate fractional-order linear time-invariant systems in general. It is also available for the degenerated case, i.e., the systems with commensurate fractional order.

Theorem 1 [62] *Consider the following n-dimensional fractional-order system,*

$$D_{0,t}^{\alpha} x(t) = Ax(t), \tag{8}$$

where $A = \left(a_{i,j}\right)_{i,j=1,2,\ldots,n}$, $\alpha \triangleq [\alpha_1, \alpha_2, \ldots, \alpha_n]$, $0 < \alpha_i < 1$. *Suppose that* M *is the lowest common multiple of the denominators* u_i*'s of* α_i*'s, where* $\alpha_i = v_i/u_i$, $(u_i, v_i) = 1$, $u_i, v_i \in \mathbb{Z}^+$ *for* $i = 1, 2, \ldots, n$.

Define $\Delta(\lambda) = \lambda^{M\alpha_i} E - A$, $i = 1, 2, \ldots, n$,

$$\Delta(\lambda) = \begin{pmatrix} \lambda^{M\alpha_1} - a_{11} & -a_{12} & \cdots & -a_{1n} \\ -a_{21} & \lambda^{M\alpha_2} - a_{22} & \cdots & -a_{2n} \\ \vdots & \vdots & \cdots & \vdots \\ -a_{n1} & -a_{n2} & \cdots & \lambda^{M\alpha_n} - a_{nn} \end{pmatrix}. \tag{9}$$

Then the zero solution of system (8) is globally asymptotically stable in the Lyapunov sense if all roots λ_i, $i = 1, 2, \ldots, n$ of the characteristic equation $\det(\Delta(\lambda)) = 0$ satisfy

$$|\arg(\lambda_i)| > \frac{\pi}{2M}. \tag{10}$$

A nonlinear FOD autonomous system with initial conditions can be described as

$$D_{0,t}^{\alpha} x(t) = F(x), \quad t \in [0, T], \quad x(0) = F(x_0), \tag{11}$$

where $0 < \alpha \le 1$, $x \in \mathbb{R}^n$. The nonlinear function $F(x) : \mathbb{R}^n \to \mathbb{R}^n$ is bounded, i.e., $F \in C^1(\Omega)$ with $F(0) = 0$. Here, $\Omega \subset \mathbb{R}$ is a bounded domain that contains the origin $x = 0$, $x_0 \in \Omega$. $D_{0,t}^{\alpha} x(t)$ denotes Caputos fractional derivative with the lower limit 0 for $F(x)$.

It is known that the necessary condition for (11) having chaotic attractors is similar to its integer-order counterpart. In a word, the equilibrium points of (11) in Ω are in the state of instability. According to (10), the necessary condition for generating chaotic attractors is mathematically equivalent to the following the instability measure for the equilibrium points in (11) [61]

$$\varpi = \frac{\pi}{2M} - \min_i \{|\arg(\lambda_i)|\}, \quad i = 1, 2, \ldots, n, \tag{12}$$

where λ_i's are roots of equations:

$$\det\left(\mathrm{diag}\left([\lambda^{M\alpha_1}, \lambda^{M\alpha_2}, \ldots, \lambda^{M\alpha_n}]\right) - \partial F/\partial x\,|_{x=x^*}\right) = 0, \quad \forall x^* \in \Omega.$$

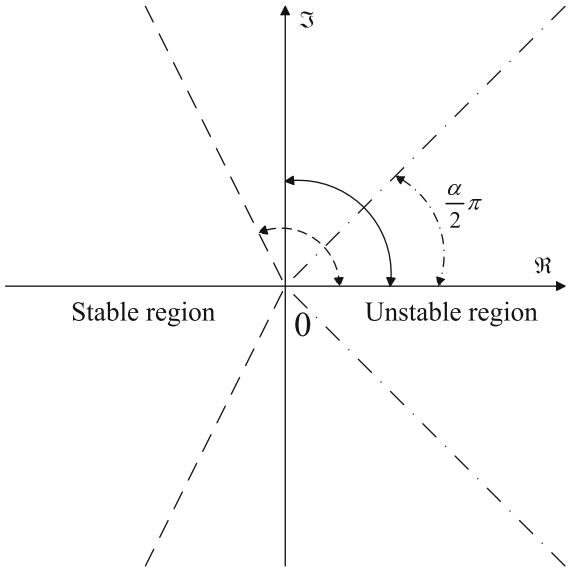

Fig. 1 The separatrices for unstable and stable regions of different fractional orders

If $\varpi < 0$, the equilibrium point x^* is asymptotic stable; otherwise, it is unstable.

Remark 1 For the commensurate fractional-order chaotic systems, $1/M = \alpha$, the condition (10) degenerates as $|\arg(\lambda_i)| > \alpha\pi/2$. The necessary condition (12) becomes $\alpha \geq (2/\pi)\min_i\{|\arg(\lambda_i)|\}$. In a special case as $\alpha = 1$, it degenerates to the stability of integer-order derivatives. In Fig. 1, the stable region and the unstable region for different fractional orders are schematically illustrated on the complex plane. The dashed lines are the separatrices of stable region and unstable region as fractional order $\alpha \in (0, 1)$. The solid line along with the imaginary axis is the separatrix for integer-order derivative. The separatrices of stable and unstable regions for $1 < \alpha < 2$ are marked with dash-dot line.

In the context of Lyapunov stability and Caputo fractional derivative, Norelys et al. [63,64], Hu et al. [65,66] proposed several new sufficient stability theorems for FOD systems very recently. They are summarized as follows:

Theorem 2 [63–66]*: Suppose that $x^* = 0$ is the equilibrium point of system (11), $0 < \alpha \leq 1$. P is a real positive-definite matrix such that the candidate function $\mathscr{H} = x^T P(D^{\alpha}_{0,t}x)$ is negative semi-definite at x^*. Then, the equilibrium point x^* is stable. Furthermore, if $\mathscr{H} < 0$, $\forall x \neq 0$, x^* is asymptotically stable.*

2.3 Some algebraic prerequisites

The following two primary algebraic lemmas are necessary to the adaptive unidirectional full-state linear feedback control scheme. They are also the fundamentals of the validation of our propositions.

Lemma 1 [67] *For any vector $x \in \mathbb{R}^{n\times 1}$, and $A = (a_{ij})_{n\times n}$ with real entries, the quadratic form x^TAx is a scalar quantity. It means that x^TAx is a real number if A is symmetric, but zero if A is skew-symmetric. $A = (a_{ij})_{n\times n}$ can be represented as a summation of a symmetric matrix $(A + A^T)/2$ (referred as the symmetric part of A) and a skew-symmetric matrix $(A - A^T)/2$ (referred as the skew-symmetric part of A). Therefore, $x^TAx = x^T((A + A^T)/2)x$ due to $x^T((A - A^T)/2)x \equiv 0$.*

Lemma 2 [68] *Suppose that $\lambda(A)$ is the eigenvalue of $A = (a_{ij})_{n\times n}$ with real entries, and $\xi = (\xi_1, \xi_2, \ldots, \xi_n)^T$ is the corresponding eigenvector of $\lambda(A)$. The real part of eigenvalues of matrix A, $\Re(\lambda(A)) = \xi^H\left((A + A^T)/2\right)\xi$, where ξ^H is the conjugate transpose of ξ, and $\xi^H\xi = 1$. Suppose that $(\lambda_1, \lambda_2, \ldots, \lambda_n)$ is the spectrum of A. Then, $(\lambda_1+\rho, \lambda_2+\rho, \ldots, \lambda_n+\rho)$ is the corresponding spectrum of summation matrix $A+\rho E$, in which ρ can be a real constant or a complex number, while E is the n-dimensional identity matrix.*

Theorem 3 *Suppose that $\bar{\lambda}_{\max}\left((A + A^T)/2\right)$ is the maximum algebraic eigenvalue of matrix $(A + A^T)/2$. Clearly, $x^TAx \leq \bar{\lambda}_{\max}\left((A + A^T)/2\right)\|x\|_2^2$, where $\|\cdot\|_2$ denotes the 2-norm of a vector x in n-dimensional Euclidean space. Furthermore,* (1) *$\bar{\lambda}_{\max}\left((A + A^T)/2\right)$ is existing and bounded if the entries a_{ij} of A is bounded, $1 \leq i, j \leq n$;* (2) *$\Re(\lambda(A)) \leq \bar{\lambda}_{\max}\left((A+A^T)/2\right)$. Obviously, $\Re(\lambda(A)) \leq \left\|(A+A^T)/2\right\|_2$.*

The proof of Theorem 3 can be seen in the "Appendix."

2.4 The synchronization scheme

System (11) is taken as the drive system. The response system is identical, but is configured with a control input vector $U_{x,y}$,

$$D^{\alpha}_{0,t}y(t) = F(y) + U_{x,y}, \quad t \in [0, T],$$
$$y(0) = F(y_0), \tag{13}$$

where $y = (y_1, y_2, \ldots, y_n)^{\mathrm{T}}$ is the state vector of the response system (13). $U_{x,y}$ is the unidirectional coupling term.

We define the error vector e as the discrepancy in variable vectors y and x, namely,

$$e = y - x. \tag{14}$$

The proposed unidirectional controller $U_{x,y}$ is in the format of linear feedback coupling,

$$U_{x,y} = K(t)(y - x) = K(t)e, \tag{15}$$

where $K(t) = \mathrm{diag}\,(k_i(t))_{n\times n}, k_i(t) \neq 0, i = 1, 2, \ldots, n$, is the coupling strength. The entries on the primary diagonal of $K(t)$ are identical, i.e., $k_i(t) = k(t), i = 1, 2, ..., n$. The feedback strength $k(t)$ will be given adaptively rather than a prescribed constant. The adaptive law is designed as following

$$\dot{k}(t) = -\gamma \|y - x\|_2^2 = -\gamma e^{\mathrm{T}} e, \tag{16}$$

where γ will be prescribed as a positive constant to regulate the convergence speed and finally, determine the coupled strength. Suppose that k_* is the upper bound, and k^* is lower bound of $k(t)$, respectively. The integer-order differential Eq. (16) will converge to a constant $k = \int_0^t \dot{k}(\tau)\mathrm{d}\tau$ once the synchronization state is achieved. It is because at this moment, $e \to 0$ as $t \to \infty$. $F(y)$ and $F(x)$ are same in structure. The dynamical difference between them can be represented as

$$F(y) - F(x) = B_{x,y}(y - x) = B_{x,y}e, \tag{17}$$

where $B_{x,y}$ is a $n \times n$ matrix that depends on vectors x and y.

The error dynamical system can be represented as

$$\begin{aligned} D_{0,t}^{\alpha} e(t) &= (F(y) - F(x) + k(t)E)\, e \\ &= \left(B_{x,y} + k(t)E\right) e. \end{aligned} \tag{18}$$

Remark 2 The proposed synchronization scheme is suitable for all of fractional-order and integer-order systems since the differential order $\alpha \in (0, 1]$. On the other hand, the synchronization can be turned into a chaos control problem if the objective state is the desired orbit. We assume that the plant system (13) is controlled to y^*, where y^* is an equilibrium point or any trajectory of the response system. It is represented as

$$\begin{aligned} &D_{0,t}^{\alpha} y(t) = F(y) + \bar{k}(t)(y - y^*) = \bar{F}(y), \quad t \in [0, T], \\ &y(0) = \bar{F}(y_0), \end{aligned} \tag{19}$$

where $\bar{k}(t)$ follows the updated law

$$\dot{\bar{k}}(t) = -\gamma \left\|y - y^*\right\|_2^2, \tag{20}$$

where the regulation factor γ is taken as before.

For a small perturbation around y^*, system (19) can be rewritten as,

$$D_{0,t}^{\alpha} y(t) = [J(y^*) + \bar{k}(t)E](y - y^*) + F(y^*), \tag{21}$$

where $J(y^*) + \bar{k}(t)E = (\partial F/\partial x)\big|_{y=y^*} + \bar{k}(t)E$ is the Jacobian matrix evaluated at y^*. The equilibrium point y^* of the controlled system (19) is locally asymptotically stable if all of the eigenvalues of the Jacobian matrix $J(y^*) + \bar{k}(t)E$ satisfy (10).

It is noticed that

$$D_{0,t}^{\alpha} y^* = F(y^*). \tag{22}$$

Defining the error $e = y - y^*$ and subtracting (22) from (21), it results in

$$\begin{aligned} D_{0,t}^{\alpha} e &= D_{0,t}^{\alpha}(y - y^*) \\ &= \left[J(y^*) + \bar{k}(t)E\right](y - y^*) \\ &= \left[J(y^*) + \bar{k}(t)E\right] e. \end{aligned} \tag{23}$$

Theorem 4 *There is a bounded constant k^* such that the error dynamical system* (18) (or (21)) *can be stabilized at the origin if all of the entries of matrix $B_{x,y}$ (or $J(y^*)$) are bounded.*

Proof Obviously, the origin is the fixed point of the error dynamical system (18). Define $e_k(t) = k(t) - k^*$. A candidate negative-definite function is chosen as,

$$\mathscr{H}(e(t), e_k(t)) = \left(e^{\mathrm{T}}(t)e_k(t)\right) P \begin{pmatrix} D_{0,t}^{\alpha} e(t) \\ \dot{k}(t) \end{pmatrix},$$

in which, $P = \mathrm{diag}(1, 1, \ldots, 1, \frac{1}{\gamma})$. Thus, we have

$$\begin{aligned} \mathscr{H}(e, e_k) &= e^{\mathrm{T}}[(B_{x,y} + k^*E)e + e_k e] - e_k e^{\mathrm{T}} e \\ &= e^{\mathrm{T}}(B_{x,y} + k^*E)e \\ &= e^{\mathrm{T}}\left(\frac{B_{x,y} + B_{x,y}^{\mathrm{T}}}{2} + k^*E\right)e \end{aligned}$$

$$\leq \left[\bar{\lambda}_{\max}\left(\frac{B_{x,y}+B_{x,y}^{\mathrm{T}}}{2}\right)+k^*\right]e^{\mathrm{T}}e$$
$$= \left[\bar{\lambda}_{\max}\left(\frac{B_{x,y}+B_{x,y}^{\mathrm{T}}}{2}\right)+k^*\right]\|e\|_2^2. \quad (24)$$

From above, the algebraic maximum eigenvalue, $\bar{\lambda}_{\max}\left((B_{x,y}+B_{x,y}^{\mathrm{T}})/2\right)$, is real and bounded if the trajectories of both drive and response systems are bounded. If $k^* \leq -\bar{\lambda}_{\max}\left((B_{x,y}+B_{x,y}^{\mathrm{T}})/2\right)$, $\mathscr{H}(e,e_k)$ is surely negative definite. Moreover, in the state of synchronization, the response system will follow the way of drive system. Therefore, the reasonable interval on which the limit value of $k(t)$ dwells for achieving synchronization is that

$$-\left|\Re\left(\lambda_{\max}\left(B_{x,y}\right)\right)-\Re\left(\lambda_{\max}\left(B_{x,x}\right)\right)\right| \geq k \geq k^*. \quad (25)$$

At the meantime, note that e_k is positive all the time, but $\dot{k}(t)$ is negative before achieving synchronization in terms of the updated law (16). In combination with Theorem 2, the error dynamical system (18) will be asymptotically stable at the origin. In this case, the synchronization states of all variables can be achieved with the adaptive linear feedback control if condition (25) is satisfied.

The proof is completed. □

Remark 3 The case for chaos control can be proved similarly if the error dynamical system (23) is involved. In fact, Theorem 4 guarantees the validity and the adaptability of the proposed synchronization (or control) scheme. It also demonstrates the flexibility of the the proposed synchronization scheme as long as the condition (25) is satisfied no matter how big e_k is. Meanwhile, it also informs us that the importance on the choice of proper regulatory factor γ, because it regulates the convergence speed and determines the ultimate feedback strength. For example, too small or too big γ should be avoid. This is because a too small γ may result in a too weak coupled strength k such that the condition (25) is not satisfied or the costing of elapsed time is too expensive. On the contrary, a too big γ may produce a too strong coupled strength k such that $k \leq k^*$. In this case, e_k will be negative such that $\mathscr{H}(e,e_k)$ is not negative definite. In the context of Theorem 2, k^* is just a expected lower bound but not a necessary condition for achieving synchronization as stated in Ref. [45].

3 Numerical simulations

3.1 Control and synchronization of FOD chaotic Lorenz system

The drive system is described as [34,35]

$$\begin{cases} \frac{\mathrm{d}^{\alpha_1}x_d}{\mathrm{d}t^{\alpha_1}} = \sigma(y_d - x_d), \\ \frac{\mathrm{d}^{\alpha_2}y_d}{\mathrm{d}t^{\alpha_2}} = -x_d z_d + \rho x_d - y_d, \\ \frac{\mathrm{d}^{\alpha_3}z_d}{\mathrm{d}t^{\alpha_3}} = x_d y_d - \beta z_d, \end{cases} \quad (26)$$

where the subscript d in x, y and z denotes that they are the variables of drive system. System (26) has three equilibrium points, one is trivial, $\mathcal{O} = (0,0,0)$, which is a saddle point of index 1 if $\rho > 1$. Another two, $\mathcal{P}^+ = (\sqrt{\beta(\rho-1)}, \sqrt{\beta(\rho-1)}, \rho-1)$ and $\mathcal{P}^- = (-\sqrt{\beta(\rho-1)}, -\sqrt{\beta(\rho-1)}, \rho-1)$ are saddle points of index 2 if $\rho > \sigma(\sigma+\beta+3)/(\sigma-\beta-1)$. These two symmetric equilibria may be surrounded by a chaotic 2-scroll attractor. Previous studies have shown that it can generate a double-scroll chaotic attractor when parameters $\sigma = 10$, $\rho = 28$, and $\beta = 8/3$ with commensurate fractional order $\alpha = 0.993$ [69] and $\alpha = 0.995$ [70], respectively. The instability measures for these two chaotic attractors are $\varpi = 1.1369 \times 10^{-6}$ and $\varpi = 1.3689 \times 10^{-6}$, respectively. With the same parameters, if the fractional orders are in-commensurate, e.g., $\alpha_1 = 0.993$, $\alpha_2 = 0.994$ and $\alpha_3 = 0.995$, respectively, $\varpi = 1.1863 \times 10^{-6} > 0$. The lowest order for generating chaotic attractors in FOD Lorenz system is 2.97 [71]. We can make an assertion that it will be a double-scroll chaotic attractor. Iterated with the Adams–Bashforth–Moulton method [72], the projection on the $x-y$ plane of the chaotic attractor is depicted in Fig. 2. Initiating from the point $x_d^{(0)} = (x_d(0), y_d(0), z_d(0)) = (10.1, 10.1, 10.1)$, its trajectory is marked with solid line after eliminating transient response. The largest Lyapunov exponent of this chaotic attractor is 1.063 by using the algorithm of small data sets [42]. Two saddle points of index 2, $\mathcal{P}^+$ and $\mathcal{P}^-$, are superimposed in the double scrolls.

System (26) can be rewritten in the form of (1),

$$\begin{pmatrix} \frac{\mathrm{d}^{\alpha_1}x_d}{\mathrm{d}t^{\alpha_1}} \\ \frac{\mathrm{d}^{\alpha_2}y_d}{\mathrm{d}t^{\alpha_2}} \\ \frac{\mathrm{d}^{\alpha_3}z_d}{\mathrm{d}t^{\alpha_3}} \end{pmatrix} = \begin{pmatrix} -\sigma & \sigma & 0 \\ \rho & -1 & 0 \\ 0 & 0 & -\beta \end{pmatrix} \begin{pmatrix} x_d \\ y_d \\ z_d \end{pmatrix} + \begin{pmatrix} 0 \\ -x_d z_d \\ x_d y_d \end{pmatrix}. \quad (27)$$

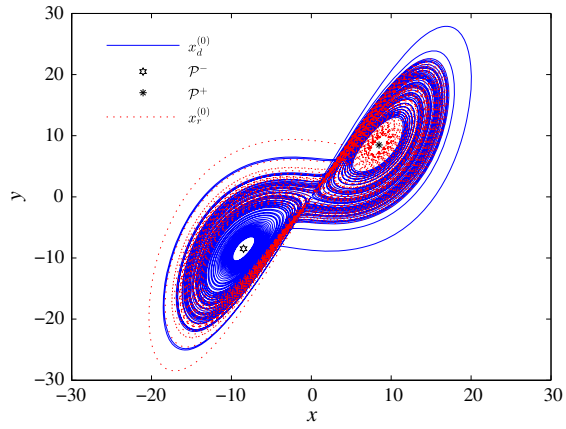

Fig. 2 Projections and two saddle points of index 2 of the FOD Lorenz system on the $x-y$ plane

The response system is configured as

$$\begin{cases} \frac{\mathrm{d}^{\alpha_1} x_r}{\mathrm{d}t^{\alpha_1}} = \sigma(y_r - x_r) + u, \\ \frac{\mathrm{d}^{\alpha_2} y_r}{\mathrm{d}t^{\alpha_2}} = -x_r z_r + \rho x_r - y_r + u, \\ \frac{\mathrm{d}^{\alpha_3} z_r}{\mathrm{d}t^{\alpha_3}} = x_r y_r - \beta z_r + u, \end{cases} \tag{28}$$

where u is the adaptive full-state linear feedback controller as designed before. Similarly rewrite the response system in the form of (1),

$$\begin{pmatrix} \frac{\mathrm{d}^{\alpha_1} x_r}{\mathrm{d}t^{\alpha_1}} \\ \frac{\mathrm{d}^{\alpha_2} y_r}{\mathrm{d}t^{\alpha_2}} \\ \frac{\mathrm{d}^{\alpha_3} z_r}{\mathrm{d}t^{\alpha_3}} \end{pmatrix} = \begin{pmatrix} -\sigma & \sigma & 0 \\ \rho & -1 & 0 \\ 0 & 0 & -\beta \end{pmatrix} \begin{pmatrix} x_r \\ y_r \\ z_r \end{pmatrix} + \begin{pmatrix} 0 \\ -x_r z_r \\ x_r y_r \end{pmatrix} + \begin{pmatrix} u \\ u \\ u \end{pmatrix}. \tag{29}$$

Without any control inputs, i.e., $u = 0$, the response system can also generate a different two-scroll chaotic attractor with another set of initial condition $x_r^{(0)} = (-0.8, -0.9, -1.0)$). The projection on the $x-y$ plane of the chaotic attractor is marked with dotted line in Fig. 2. The maximal eigenvalue $\bar{\lambda}(J(y))_{\max}$ of this chaotic attractor is real, $\bar{\lambda}(J(y))_{\max} = 10.0651$, and $\bar{\lambda}_{\max}((J(y) + J^{\mathrm{T}}(y))/2) = 11.9244$. As stated as before, such a two-scroll chaotic attractor can be controlled to a desired state. Hereby, the error dynamical system (23) is involved. It is described precisely as

$$\begin{aligned} D_{0,t}^{\alpha} e &= [J(y^*) + \bar{k}(t)E]e \\ &= \left[\begin{pmatrix} -\sigma & \sigma & 0 \\ \rho - z_r & -1 & -x_r \\ y_r & x_r & -\beta \end{pmatrix}_{y^*} + \begin{pmatrix} \bar{k}(t) & 0 & 0 \\ 0 & \bar{k}(t) & 0 \\ 0 & 0 & \bar{k}(t) \end{pmatrix} \right] e. \end{aligned} \tag{30}$$

Table 1 $\Re(\lambda(J(y^*)))_{\max}$, $\bar{k}$ and $\bar{k}(t)$ for different equilibria

Equilibria	$\Re(\lambda(J(y^*)))_{\max}$	$\bar{k}$	$\bar{k}(t)$
$\mathcal{O}$	11.8277	−11.8277	−11.8825
$\mathcal{P}^+$	0.094	−0.1954	−2.1692
$\mathcal{P}^-$	0.094	−0.1954	−0.2855

In the following illustrations, three equilibria $\mathcal{O}$, $\mathcal{P}^+$, and $\mathcal{P}^-$ are taken as the desired state, respectively. The relations of $\Re(\lambda(J(y^*)))_{\max}$, the necessary control strength $\bar{k}$ and the maximal updated control strength $\bar{k}(t)$ for different equilibria are shown in Table 1. The eigenvalues of the simultaneous equilibria $\mathcal{P}^+$ and $\mathcal{P}^-$ are same. Two conjugate eigenvalues have positive real part, $\lambda_{1,2}(J(y^*)) = 0.094 \pm 10.1945i$. Figure 3a–c present the control effects as $\gamma = 0.1$. It is worth noticing that the actual costs of control to $\mathcal{P}^+$ and $\mathcal{P}^-$ are not same due to different control inputs. The evaluations of $\bar{k}(t)$ as γ varying in the interval $(0, 0.2]$ for different control objectives are shown in Fig. 3d.

In synchronization, the error dynamical system can also be represented in the format of (1),

$$\begin{aligned} \begin{pmatrix} \frac{\mathrm{d}^{\alpha_1} e_x}{\mathrm{d}t^{\alpha_1}} \\ \frac{\mathrm{d}^{\alpha_2} e_y}{\mathrm{d}t^{\alpha_2}} \\ \frac{\mathrm{d}^{\alpha_3} e_z}{\mathrm{d}t^{\alpha_3}} \end{pmatrix} &= \left[\begin{pmatrix} -\sigma & \sigma & 0 \\ \rho & -1 & 0 \\ 0 & 0 & -\beta \end{pmatrix} + \begin{pmatrix} 0 & 0 & 0 \\ -z_r & 0 & -x_d \\ y_d & x_r & 0 \end{pmatrix} \right. \\ &\quad \left. + k(t) \begin{pmatrix} 1 & 0 & 0 \\ 0 & 1 & 0 \\ 0 & 0 & 1 \end{pmatrix} \right] \begin{pmatrix} e_x \\ e_y \\ e_z \end{pmatrix} \\ &= (A + B_{x,y} + k^* E)e + (k(t) - k^*)e. \end{aligned} \tag{31}$$

where the identity matrix $E \in \mathbb{R}^{3\times 3}$.

$$\frac{A + A^{\mathrm{T}}}{2} = \begin{pmatrix} -\sigma & \frac{\sigma+\rho}{2} & 0 \\ \frac{\sigma+\rho}{2} & -1 & 0 \\ 0 & 0 & -\beta \end{pmatrix},$$

$$\frac{B_{x,y} + B_{x,y}^{\mathrm{T}}}{2} = \begin{pmatrix} 0 & -\frac{z_r}{2} & \frac{y_d}{2} \\ -\frac{z_r}{2} & 0 & \frac{x_r - x_d}{2} \\ \frac{y_d}{2} & \frac{x_r - x_d}{2} & 0 \end{pmatrix}.$$

It is easy to obtain the maximal eigenvalue of $(A + A^{\mathrm{T}})/2$ is 14.0256. It can be found that $\bar{\lambda}_{\max}\big((B_{x,y} + B_{x,y}^{\mathrm{T}})/2\big) = 28.0887$ by numerical computing all of the eigenvalues of matrix $(B_{x,y} + B_{x,y}^{\mathrm{T}})/2$ along with the attractors starting from different initial points, $x_d^{(0)}$

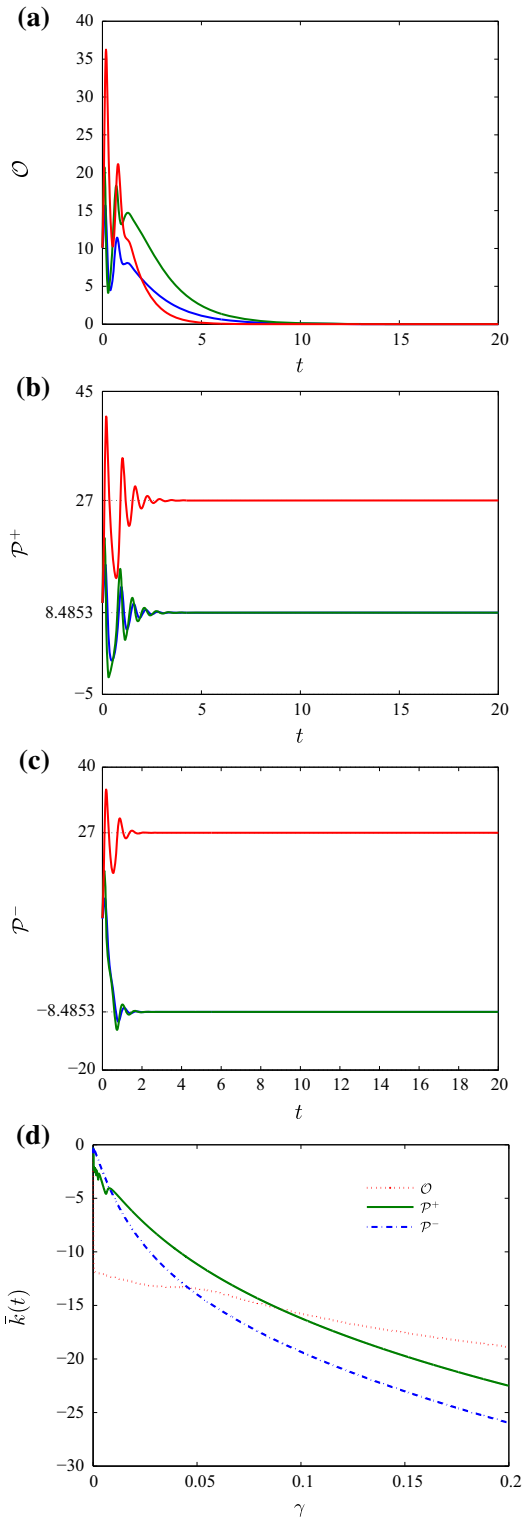

Fig. 3 Numerical results of the control effects. **a** Controlled to $\mathcal{O}$, **b** controlled to $\mathcal{P}^+$, **c** controlled to $\mathcal{P}^-$, **d** the evaluations of $\bar{k}(t)$ as γ varying

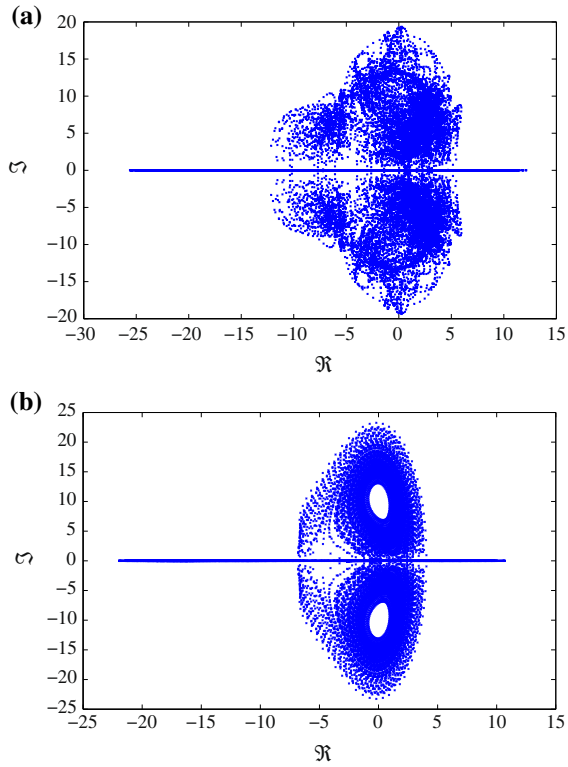

Fig. 4 The respective distribution of eigenvalues in initial regime and synchronization regime. **a** In initial regime, **b** in synchronization regime

and $x_r^{(0)}$. Without loss of generality, k^* will be set a value slightly lower than $-\bar{\lambda}_{\max}\left((A+A^{\mathrm{T}})/2\right) - \bar{\lambda}_{\max}\left((B_{x,y}+B_{x,y}^{\mathrm{T}})/2\right)$, e.g., $k^* = -42.5$. In Fig. 4a, all of the numerical eigenvalues of the objective matrix $A + B_{x,y}$ is plotted on their complex plane. The maximum eigenvalue is real, $\bar{\lambda}_{\max}\left(A + B_{x,y}\right) = 12.1391$. In the synchronization regime, the distribution of all of numerical eigenvalues of the objective matrix $A + B_{x,x}$ is presented in Fig. 4b. The maximum eigenvalue is also real, $\lambda_{\max}\left(A + B_{x,x}\right) = 10.6709$. It means that the maximum eigenvalue should be reduced by at least 1.7996. Therefore, the error dynamical system can be stabilized once the feedback strength $k^* \le k \le -1.7996$. We restrict the elapsed time for achieving synchronization is 50 with fixed time-step 0.001, and sufficient iteration time 10^5. The synchronization errors are monitored by the root-mean-square error (RMSE) in variables, RMSE $= \sqrt{e^{\mathrm{T}}e/n}$. The relationship of ultimate control strength k and γ is plotted in Fig. 5. The γ values before vertical dashed line are unacceptable

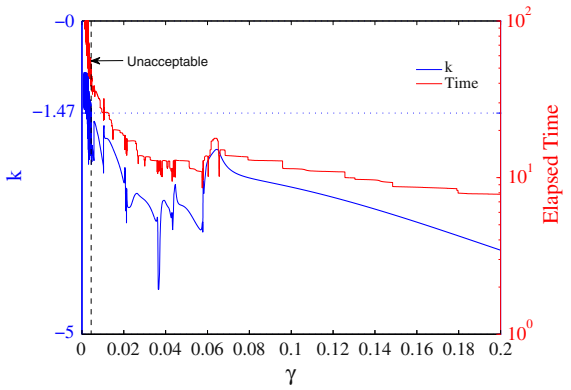

Fig. 5 The evaluations of $k(t)$, and the elapsed time versus different γ of the FOD Lorenz system

because RMSE we monitored is not lower than what we expected (10^{-4}), in the restricted elapsed time. The effectiveness of the errors in variables is illustrated in Fig. 6 when $\gamma = 0.001$. Therefore, to avoid long-time running and big feedback strengths, the suggested interval for regulation factor γ is [0.001, 0.2].

3.2 Synchronization of FOD chaotic Rössler system

The Rössler system is the simplest three-dimensional nonlinear system that can produce screw-type and spiral-type chaotic attractor [73]. Its chaotic attractor belongs to the 1-scroll attractor family. The equations of the drive system are [14],

$$\begin{cases} \frac{\mathrm{d}^{\alpha_1} x_d}{\mathrm{d}t^{\alpha_1}} = -(y_d + z_d), \\ \frac{\mathrm{d}^{\alpha_2} y_d}{\mathrm{d}t^{\alpha_2}} = x_d + a y_d, \\ \frac{\mathrm{d}^{\alpha_3} z_d}{\mathrm{d}t^{\alpha_3}} = b + z_d(x_d - c). \end{cases} \tag{32}$$

System (32) satisfies the necessary condition for exhibiting one-scroll chaotic attractor when the parameters $(a, b, c) = (0.63, 0.2, 10)$ and fractional orders $(\alpha_1, \alpha_2, \alpha_3) = (0.9, 0.8, 0.7)$ [74].

The response system is configured as

$$\begin{cases} \frac{\mathrm{d}^{\alpha_1} x_r}{\mathrm{d}t^{\alpha_1}} = -(y_r + z_r) + u, \\ \frac{\mathrm{d}^{\alpha_2} y_r}{\mathrm{d}t^{\alpha_2}} = x_r + 0.63 y_r + u, \\ \frac{\mathrm{d}^{\alpha_3} z_r}{\mathrm{d}t^{\alpha_3}} = 0.2 + z_r(x_r - 10) + u, \end{cases} \tag{33}$$

where u is the adaptive linear feedback controller as (15).

Note that the Rössler system cannot be represented as (1), but its linearly coupling error dynamical system

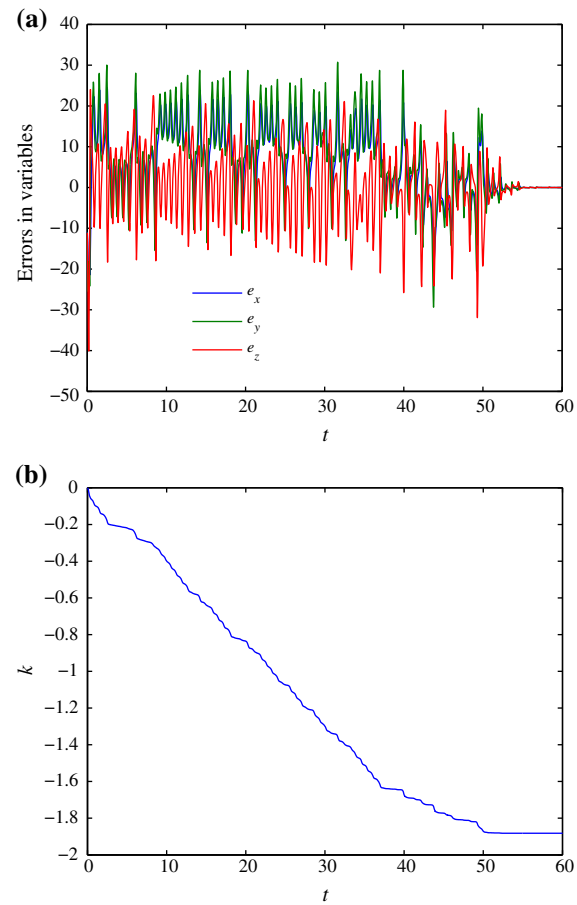

Fig. 6 Numerical results of the scheme on linearly coupled FOD Lorenz systems when $\gamma = 0.001$. **a** The errors in variables, **b** the evaluation of $k(t)$

can [24]. Rewrite the error dynamical system in the form of (1), which reads

$$\begin{aligned} \begin{pmatrix} \frac{\mathrm{d}^{\alpha_1} e_x}{\mathrm{d}t^{\alpha_1}} \\ \frac{\mathrm{d}^{\alpha_2} e_y}{\mathrm{d}t^{\alpha_2}} \\ \frac{\mathrm{d}^{\alpha_3} e_z}{\mathrm{d}t^{\alpha_3}} \end{pmatrix} &= \left[\begin{pmatrix} 0 & -1 & -1 \\ 1 & 0.63 & 0 \\ 0 & 0 & -10 \end{pmatrix} + \begin{pmatrix} z_d & 0 & 0 \\ 0 & 0 & 0 \\ 0 & 0 & x_r \end{pmatrix} \right. \\ &\quad \left. + k(t) \begin{pmatrix} 1 & 0 & 0 \\ 0 & 1 & 0 \\ 0 & 0 & 1 \end{pmatrix} \right] \begin{pmatrix} e_x \\ e_y \\ e_z \end{pmatrix} \\ &= (A + B_{x,y} + k^* E)e + (k(t) - k^*)e. \end{aligned} \tag{34}$$

where the identity matrix $E \in \mathbb{R}^{3\times 3}$.

$$\frac{A + A^{\mathrm{T}}}{2} = \begin{pmatrix} 0 & 0 & -\frac{1}{2} \\ 0 & 0.63 & 0 \\ -\frac{1}{2} & 0 & -10 \end{pmatrix},$$

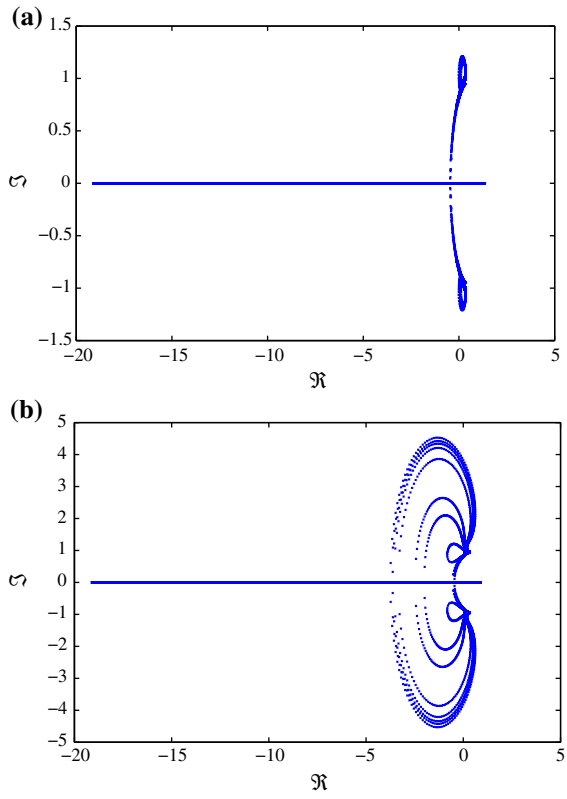

Fig. 7 The respective distribution of eigenvalues in initial regime and synchronization regime. **a** In initial regime, **b** in synchronization regime

$$\frac{B_{x,y}+B_{x,y}^{\mathrm{T}}}{2}=\begin{pmatrix}0 & 0 & \frac{z_r}{2}\\ 0 & 0 & 0\\ \frac{z_r}{2} & 0 & x_d\end{pmatrix}.$$

It easy to get $\bar{\lambda}_{\max}\left((A+A^{\mathrm{T}})/2\right)=0.63$. The eigenvalues of matrix $(B_{x,y}+B_{x,y}^{\mathrm{T}})/2$ are calculated along with the attractors starting from different initial points $x_d^{(0)}$, $x_r^{(0)}$ as before. The numerical result is $\bar{\lambda}_{\max}\left((B_{x,y}+B_{x,y}^{\mathrm{T}})/2\right)=11.4254$. Then $k^*\leq -12.0554$. In the initial regime of drive system (32) and response system (33), $\lambda_{\max}\left(A+B_{x,y}\right)=1.3585$. In the synchronization regime, $y\to x$, $\lambda_{\max}\left(A+B_{x,x}\right)=0.8869$. The numerical results of all of the eigenvalues of FOD Rössler system are shown in Fig. 7a, b. Thus, the expected evolutions of $k(t)$ had better fall into the interval $[-12.0554,-0.4716]$ for successful synchronization via unidirectional full-state adaptive linear feedback control. In Fig. 8, the corresponding evolutions of $k(t)$ and the elapsed time are plotted against the suggested regulation factors γ dynamically.

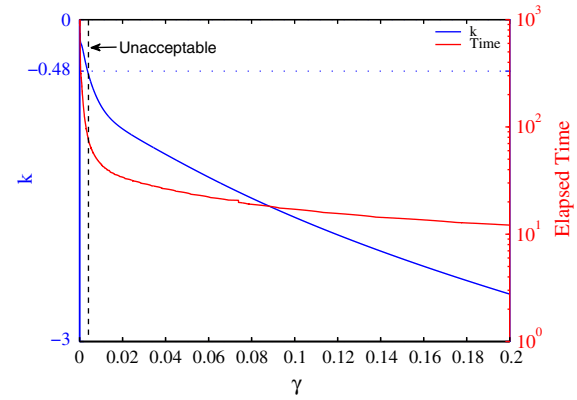

Fig. 8 The evaluations of $k(t)$ and the elapsed time versus different γ of the FOD Rössler system

3.3 Synchronization of FOD chaotic Liu system

Both the Liu system and its linearly coupling error dynamical system cannot be represented as (1) [39–42]. The incommensurate fractional-order model of Liu system is rewritten as

$$\begin{cases}\frac{\mathrm{d}^{\alpha_1}x_d}{\mathrm{d}t^{\alpha_1}}=-ax_d-\tilde{a}y_d^2,\\ \frac{\mathrm{d}^{\alpha_2}y_d}{\mathrm{d}t^{\alpha_2}}=by_d-\tilde{m}x_dz_d,\\ \frac{\mathrm{d}^{\alpha_3}z_d}{\mathrm{d}t^{\alpha_3}}=-cz_d+mx_dy_d.\end{cases}\tag{35}$$

It has been reported that the lowest order for existing chaotic attractor in the case of commensurate orders is 2.76, whereas in the incommensurate case is 2.60 [41]. The parameter values of the fractional-order Liu system are set as $a=\tilde{a}=1$, $b=2.5$, $m=\tilde{m}=4$ and $c=5$ to ensure the chaotic motion with incommensurate fractional orders $\alpha_1=0.98$, $\alpha_2=\alpha_3=0.95$.

The response system is configured as

$$\begin{cases}\frac{\mathrm{d}^{\alpha_1}x_r}{\mathrm{d}t^{\alpha_1}}=-ax_r-\tilde{a}y_r^2+k(t)(x_r-x_d),\\ \frac{\mathrm{d}^{\alpha_2}y_r}{\mathrm{d}t^{\alpha_2}}=by_r-\tilde{m}x_rz_r+k(t)(y_r-y_d),\\ \frac{\mathrm{d}^{\alpha_3}z_r}{\mathrm{d}t^{\alpha_3}}=-cz_r+mx_ry_r+k(t)(z_r-z_d),\end{cases}\tag{36}$$

where $k(t)$ follows the update law (16).

The error dynamical system between them is

$$\begin{aligned}\begin{pmatrix}\frac{\mathrm{d}^{\alpha_1}e_x}{\mathrm{d}t^{\alpha_1}}\\ \frac{\mathrm{d}^{\alpha_2}e_y}{\mathrm{d}t^{\alpha_2}}\\ \frac{\mathrm{d}^{\alpha_3}e_z}{\mathrm{d}t^{\alpha_3}}\end{pmatrix}&=\left[\begin{pmatrix}-1 & -(y_r+y_d) & 0\\ -4z_r & 2.5 & -4x_d\\ y_r & x_d & -5\end{pmatrix}\right.\\ &\quad\left.+k(t)\begin{pmatrix}1 & 0 & 0\\ 0 & 1 & 0\\ 0 & 0 & 1\end{pmatrix}\right]\begin{pmatrix}e_x\\ e_y\\ e_z\end{pmatrix}\\ &=(B_{x,y}+k(t)^*E)e,\end{aligned}\tag{37}$$

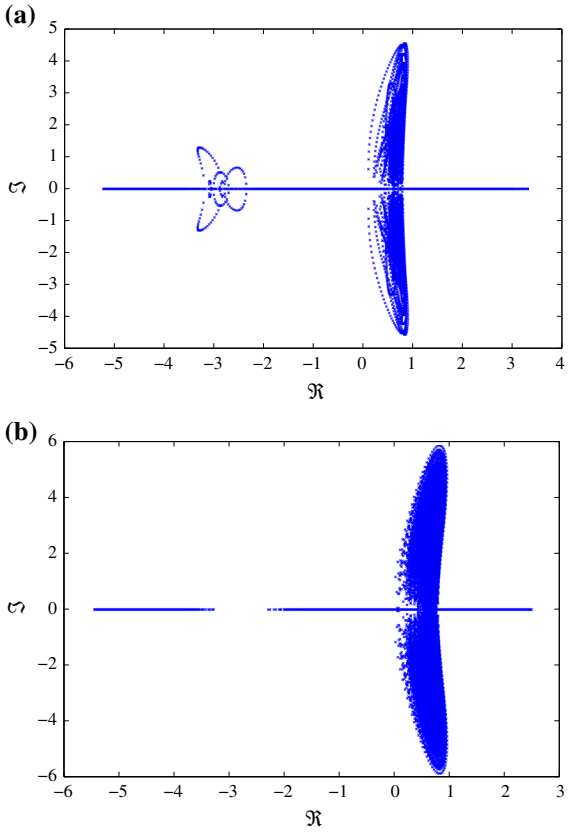

Fig. 9 The respective distribution of eigenvalues in initial regime and synchronization regime. **a** In initial regime, **b** in synchronization regime

where the identity matrix $E \in \mathbb{R}^{3\times 3}$.

$$\frac{B_{x,y} + B_{x,y}^{\mathrm{T}}}{2} = \begin{pmatrix} -1 & -2z_r - \frac{y_r+y_d}{2} & \frac{y_r}{2} \\ -2z_r - \frac{y_r+y_d}{2} & 2.5 & -\frac{3}{2}x_d \\ \frac{y_r}{2} & -\frac{3}{2}x_d & -5 \end{pmatrix}.$$

The initial conditions still are $x_d^{(0)}$ and $x_r^{(0)}$. $\bar{\lambda}_{\max}\left((B_{x,y} + B_{x,y}^{\mathrm{T}})/2\right) = 5.0871$ after long-time computations. In the initial regime, Fig. 9a shows $\lambda_{\max}\left(B_{x,y}\right) = 3.2891$. While in the synchronization regime, as shown in Fig. 9b, $\lambda_{\max}\left(B_{x,x}\right) = 2.4938$. Therefore, the expected evolutions of $k(t)$ had better fall into the interval $[-5.0871, -0.7953]$ for successful synchronization. In Fig. 9, the corresponding evolutions of $k(t)$ and elapsed time are plotted against the regulation factors γ dynamically. Too small γ values (the values before the vertical dashed line in Fig. 10) are

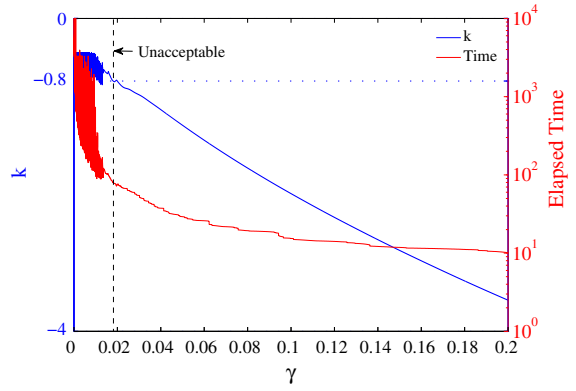

Fig. 10 The evaluations of $k(t)$, and the elapsed time versus different γ of the FOD Liu system

not acceptable because the chaotic Liu attractor has a long-time transient response starting from $x_d^{(0)}$.

4 Conclusions

In this paper, an adaptive synchronization scheme designed with full-state linear error feedback is proposed for general FOD chaotic systems. Rigorous theoretical and numerical results have been presented to demonstrate the effectiveness. Synchronization of two identical FOD chaotic systems with a unidirectional full-state linear feedback coupling can be achieved effectively if the ultimate adaptive feedback strengths fall into the suggested interval of regulation factor. It is believed that the proposed synchronization scheme is useful for realizing in practice due to their simple interactions.

However, it should be noted that the stability region of the error system is constraint on the left-half part only of a differential equation with fractional-order α, and α should be in the interval of $(0, 1]$. In other words, the two stability regions between the imaginary axis and the unstable region are never considered due to the limitation of Theorem 2. Moreover, the intervention of system $\mathscr{H}$ in some way restraints the adaptive control scheme in extension to different synchronization. In this sense, the present scheme loses sight of the fact that a FOD system has a wider stable amplitude region in comparison with its integer-order counterpart. In addition, the upper bound of the evolutions of $k(t)$ is closely related to the precision of the adopted numerical algorithm of FOD systems. The regulatory

factor γ in the adaptive law for every linear-coupled FOD chaotic systems can be optimized only from a posteriori approach. On the other hand, this bound is just a difference of maximum eigenvalues in the initial regime and the synchronization regime of an identical FOD chaotic system starting from different initial condition. In comparison with the results of [42,50], the upper bound we obtained may be compact or loose. Thus, how to adjust the complex eigenvalues of a FOD system into the amplitude region, in which the error dynamical system will be asymptotic stable, is worth going on. Moreover, the optimization on the present adaptive linear error coupling scheme will be studied further, such as, bidirectional coupling [75] and partial coupling [76,77].

Acknowledgments The research was supported by NNSFs of China (Grant Nos. 11161027, 11262009), Key FSN of Gansu Province, China (Grant No. 1104WCGA195), and the Specialized RF for the Doctoral Program of Higher Education of China (Grant No. 20136204110001).

Appendix: The proof of Theorem 3

Proof A symmetric matrix has exactly n real eigenvalues (counting multiplicities). There is an orthogonal matrix Q, such that

$$Q^{\mathrm{T}}\left(\frac{A+A^{\mathrm{T}}}{2}\right)Q=\bar{\Lambda}=\left(\bar{\lambda}_1,\bar{\lambda}_2,\ldots,\bar{\lambda}_n\right),$$

where $\bar{\Lambda}$ is the spectrum of the symmetric part of A, and $\bar{\lambda}_i\in\mathbb{R}$, $i=1,2,\ldots,n$.

Due to

$$\bar{\lambda}_{\max}\left(\frac{A+A^{\mathrm{T}}}{2}\right)=\max\left\{\bar{\lambda}_1,\bar{\lambda}_2,\ldots,\bar{\lambda}_n\right\},$$

and

$$\bar{\lambda}_{\max}\left(\frac{A+A^{\mathrm{T}}}{2}\right)=\max_{x\neq 0}\frac{x^{\mathrm{T}}\left(\frac{A+A^{\mathrm{T}}}{2}\right)x}{x^{\mathrm{T}}x},$$

one has

$$\bar{\lambda}_{\max}\left(\frac{A+A^{\mathrm{T}}}{2}\right)\geq\frac{u^{\mathrm{T}}\left(\frac{A+A^{\mathrm{T}}}{2}\right)u}{u^{\mathrm{T}}u}.$$

Let $u^{\mathrm{T}}=(1,1,\ldots,1)$,

$$\begin{aligned}\bar{\lambda}_{\max}\left(\frac{A+A^{\mathrm{T}}}{2}\right)&\geq u^{\mathrm{T}}\left(\frac{A+A^{\mathrm{T}}}{2}\right)u\\&=\sum_{ij}^{n}\left(\frac{a_{ij}+a_{ji}}{2}\right).\end{aligned}$$

On the other hand, according to the Gershgorin's circle theorem, we have

$$\bar{\lambda}_{\max}\left(\frac{A+A^{\mathrm{T}}}{2}\right)\leq\sum_{i\neq j}^{n}\left(\frac{\left|a_{ij}+a_{ji}\right|}{2}\right)+a_{ii}.$$

Suppose q_i is the ith column of Q,

$$\begin{aligned}\|x\|_2^2=x^{\mathrm{T}}x&=x^{\mathrm{T}}QQ^{\mathrm{T}}x=\left(Q^{\mathrm{T}}x\right)^{\mathrm{T}}\left(Q^{\mathrm{T}}x\right)\\&=\sum_{i=1}^{n}\left(q_i^{\mathrm{T}}x\right)^2.\end{aligned}$$

And,

$$\begin{aligned}x^{\mathrm{T}}Ax&=x^{\mathrm{T}}\left(\frac{A+A^{\mathrm{T}}}{2}\right)x=x^{\mathrm{T}}\left(Q\bar{\Lambda}Q^{\mathrm{T}}\right)x\\&=\left(Q^{\mathrm{T}}x\right)^{\mathrm{T}}\bar{\Lambda}\left(Q^{\mathrm{T}}x\right)\\&=\sum_{i=1}^{n}\bar{\lambda}_i\left(q_i^{\mathrm{T}}x\right)^2\leq\max_i(\bar{\lambda}_i)\sum_{i=1}^{n}\left(q_i^{\mathrm{T}}x\right)^2\\&=\bar{\lambda}_{\max}\left(\frac{A+A^{\mathrm{T}}}{2}\right)\|x\|_2^2.\end{aligned}$$

Next, $\Re(A)=\xi^{\mathrm{H}}\left((A+A^{\mathrm{T}})/2\right)\xi=\xi^{\mathrm{H}}\left(Q\bar{\Lambda}Q^{\mathrm{T}}\right)\xi$. Denotes that $y=Q\xi=(y_1,y_2,\ldots,y_n)^{\mathrm{T}}$. Obviously, $y^{\mathrm{H}}y=1$ and $\Re(A)=\bar{\lambda}_1|y_1|^2+\bar{\lambda}_2|y_2|^2+\cdots+\bar{\lambda}_n|y_n|^2$.

Therefore,

$$\begin{aligned}\Re(A)&\leq\bar{\lambda}_{\max}\left(\frac{A+A^{\mathrm{T}}}{2}\right)\left(|y_1|^2+|y_2|^2+\cdots+|y_n|^2\right)\\&=\bar{\lambda}_{\max}\left(\frac{A+A^{\mathrm{T}}}{2}\right).\end{aligned}$$

Obviously,

$$\Re(A)\leq\left\|\frac{A+A^{\mathrm{T}}}{2}\right\|_2,$$

because the spectral radius ρ of a symmetric matrix satisfies,

$$\bar{\lambda}_{\max}\left(\frac{A+A^{\mathrm{T}}}{2}\right)\leq\rho\left(\frac{A+A^{\mathrm{T}}}{2}\right)\leq\left\|\frac{A+A^{\mathrm{T}}}{2}\right\|_2.$$

This is the end of the proof. □

References

1. Ott, E., Grebogi, C., Yorke, J.A.: Controlling chaos. Phys. Rev. Lett. **64**, 1196–1199 (1990)
2. Pecora, L.M., Carroll, T.L.: Synchronization in chaotic systems. Phys. Rev. Lett. **64**, 821–824 (1990)

3. Boccaletti, S., Kurths, J., Osipovd, G., Valladares, D.L., Zhou, C.S.: The synchronization of chaotic systems. Phys. Rep. **366**, 1–101 (2002)
4. Deng, T., Xia, G.Q., Wu, Z.M.: Broadband chaos synchronization and communication based on mutually coupled VCSELs subject to a bandwidth-enhanced chaotic signal injection. Nonlinear Dyn. **76**, 399–407 (2014)
5. Zhu, Q.X., Cao, J.D.: Adaptive synchronization of chaotic Cohen Crossberg neural networks with mixed time delays. Nonlinear Dyn. **61**, 517–534 (2010)
6. Mohammad, P.A., Hasan, P.A.: Robust synchronization of a chaotic mechanical system with nonlinearities in control inputs. Nonlinear Dyn. **73**, 363–376 (2013)
7. Volos, C.K., Kyprianidis, I.M., Stouboulos, I.N.: Image encryption process based on chaotic synchronization phenomena. Signal Process **93**, 1328–1340 (2013)
8. Chen, D.Y., Zhang, R.F., Ma, X.Y., Liu, S.: Chaotic synchronization and anti-synchronization for a novel class of multiple chaotic systems via a sliding mode control scheme. Nonlinear Dyn. **69**, 35–55 (2012)
9. Aghababa, M.P., Heydari, A.: Chaos synchronization between two different chaotic systems with uncertainties, external disturbances, unknown parameters and input nonlinearities. Appl. Math. Model. **36**, 1639–1652 (2012)
10. Zhao, J.K., Wu, Y., Wang, Y.Y.: Generalized finite-time synchronization between coupled chaotic systems of different orders with unknown parameters. Nonlinear Dyn. **74**, 479–485 (2013)
11. Yang, C.C., Lin, C.L.: Robust adaptive sliding mode control for synchronization of space-clamped FitzHugh-Nagumo neurons. Nonlinear Dyn. **69**, 2089–2096 (2012)
12. Sun, Y.J.: Generalized projective synchronization for a class of chaotic systems with parameter mismatching, unknown external excitation, and uncertain input nonlinearity. Commun. Nonlinear Sci. Numer. Simul. **16**, 3863–3870 (2011)
13. Baziliauskas, A., Krivickas, R., Tamasevicius, A.: Coupled chaotic Colpitts oscillator: identical and mismatched cases. Nonlinear Dyn. **44**, 151–158 (2006)
14. Li, C.G., Chen, G.R.: Chaos and hyperchaos in the fractional-order Rössler equations. Phys. A **341**, 55–61 (2004)
15. Agrawal, S.K., Das, S.: A modified adaptive control method for synchronization of some fractional chaotic systems with unknown parameters. Nonlinear Dyn. **73**, 907–919 (2013)
16. Wang, Z., Huang, X., Zhao, Z.: Synchronization of nonidentical chaotic fractional-order systems with different orders of fractional derivatives. Nonlinear Dyn. **69**, 999–1007 (2012)
17. Caponetto, R., Dongola, G., Fortuna, L., Petráš, I.: Fractional Order Systems: Modeling and Control Applications. World Scientific Publishing, Singapore (2010)
18. Muthukumar, P., Balasubramaniam, P.: Feedback synchronization of the fractional order reverse butterfly-shaped chaotic system and its application to digital cryptography. Nonlinear Dyn. **74**, 1169–1181 (2013)
19. Muthukumar, P., Balasubramaniam, P., Ratnavelu, K.: Synchronization and an application of a novel fractional order King Cobra chaotic system. Chaos **24**, 033105 (2014)
20. Xu, Y., Wang, H., Li, Y.G., Pei, B.: Image encryption based on synchronization of fractional chaotic systems. Commun. Nonlinear Sci. Numer. Simul. **19**, 3735–3744 (2014)
21. Yu, H.J., Liu, Y.Z.: Chaotic synchronization based on stability criterion of linear systems. Phys. Lett. A **314**, 292–298 (2003)
22. Wu, X.F., Chen, G.R., Cai, J.P.: Chaos synchronization of the master–slave generalized Lorenz systems via linear state error feedback control. Phys. D **229**, 52–80 (2007)
23. Jiang, G.P., Tang, K.S., Chen, G.R.: A simple global synchronization criterion for coupled chaotic systems. Chaos Solitons Fractals **15**, 925–935 (2003)
24. Jiang, G.P., Tang, K.S.: A simple global synchronization criterion for coupled chaotic systems via unidirectional linear error feedback approach. Int. J. Bifurc. Chaos **12**, 2239–2263 (2002)
25. Li, C.D., Liao, X.F.: Anti-synchronization of a class of coupled chaotic systems via linear feedback control. Int. J. Bifurc. Chaos **16**, 2041–2047 (2006)
26. Lü, J.H., Zhou, T.S., Zhang, S.C.: Chaos synchronization between linearly coupled chaotic systems. Chaos Solitons Fractals **14**, 529–541 (2002)
27. Liu, F., Ren, Y., Shan, X.M., Qiu, Z.L.: A linear feedback synchronization theorem for a class of chaotic systems. Chaos Solitons Fractals **13**, 723–730 (2002)
28. Yan, Z.Y., Yu, P.: Linear feedback control, adaptive feedback control and their combination for chaos (lag) synchronization of LC chaotic systems. Chaos Solitons Fractals **33**, 419–435 (2007)
29. Odibat, Z.M.: Adaptive feedback control and synchronization of non-identical chaotic fractional order systems. Nonlinear Dyn. **60**, 479–487 (2010)
30. Hadhrami, S.A., Saaban, A.B., Ibrahim, A.B., Shahzad, M., Ahmad, I.: Linear active control algorithm to synchronize a nonlinear HIV/AIDS dynamical system. Asian J. Appl. Sci. Eng. **3**, 96–113 (2014)
31. Saaban, A.B., Ibrahim, A.B., Shahzad, M., Ahmad, I.: Identical synchronization of a new chaotic system via nonlinear control and linear active control techniques: a comparative analysis. Int. J. Hybrid Inf. Technol. **7**, 211–224 (2014)
32. Zhang, F.R., Chen, G.R., Li, C.P., Kurths, J.: Chaos synchronization in fractional differential systems. Phil. Trans. R. Soc. A **371**, 20120155 (2013)
33. Gammoudi, I.E., Feki, M.: Synchronization of integer order and fractional order Chua's systems using robust observer. Commun. Nonlinear Sci. Numer. Simul. **18**, 625–638 (2013)
34. Chen, D.Y., Zhang, R.F., Sprott, J.C., Chen, H.T., Ma, X.Y.: Synchronization between integer-order chaotic systems and a class of fractional-order chaotic systems via sliding mode control. Chaos **22**, 023130 (2012)
35. Zhou, P., Cheng, Y.M., Kuang, F.: Synchronization between fractional-order chaotic systems and integer orders chaotic systems (fractional-order chaotic systems). Chin. Phys. B **19**, 090503 (2010)
36. Xu, F.: Integer and fractional order multiwing chaotic attractors via the Chen system and the Lü system with switching controls. Int. J. Bifurc. Chaos **24**, 1450029 (2014)
37. Deng, W.H., Li, C.P.: Chaos synchronization of the fractional Lü system. Phys. A **353**, 61–72 (2005)
38. Wu, X.J., Li, J., Chen, G.R.: Chaos in the fractional order unified system and its synchronization. J. Frankl. Inst. **345**, 392–401 (2008)

39. Liu, C.X., Liu, L., Liu, T.: A novel three-dimensional autonomous chaos system. Chaos Solitons Fractals **39**, 1950–1958 (2009)
40. Liu, C.X., Liu, T., Liu, L., Liu, K.: A new chaotic attractor. Chaos Solitons Fractals **22**, 1031–1038 (2004)
41. Daftardar-Gejji, V., Bhalekar, S.: Chaos in fractional ordered Liu system. Comput. Math. Appl. **59**, 1117–1127 (2010)
42. Wang, X.Y., Wang, M.J.: Dynamic analysis of the fractional-order Liu system and its synchronization. Chaos **17**, 033106 (2007)
43. Li, X.F., Chu, Y.D., Zhang, J.G., Chang, Y.X.: Nonlinear dynamics and circuit implementation for a new Lorenz-like attractor. Chaos Solitons Fractals **41**, 2360–2370 (2009)
44. Nyamoradi, N., Javidi, M.: Sliding mode control of uncertain unified chaotic fractional-order new Lorenz-like system. Dyn. Cont. Disc. Impul. Syst. **20**, 63–82 (2013)
45. Zhang, R.X., Yang, S.P.: Adaptive synchronization of fractional-order chaotic systems. Chin. Phys. B **19**, 020510 (2010)
46. Restrepo, J.G., Ott, E., Hunt, B.R.: Spatial patterns of desynchronization bursts in networks. Phys. Rev. E **69**, 066215 (2004)
47. Yanchuka, S., Maistrenkoa, Y., Mosekilde, E.: Loss of synchronization in coupled Rössler systems. Phys. D **154**, 26–42 (2001)
48. Wu, Y., Liu, W.P., Xiao, J.H., Zhan, M.: Chaos desynchronization in strongly coupled systems. Phys. Lett. A **369**, 464–468 (2007)
49. Acharyya, S., Amritkar, R.E.: Desynchronization bifurcation of coupled nonlinear dynamical systems. Chaos **21**, 023113 (2011)
50. Wang, F.Q., Liu, C.X.: A new criterion for chaos and hyperchaos synchronization using linear feedback control. Phys. Lett. A **360**, 274–278 (2006)
51. Huang, D.B.: Synchronization-based estimation of all parameters of chaotic systems from time series. Phys. Rev. E **69**, 067201 (2004)
52. Huang, D.B.: Simple adaptive-feedback controller for identical chaos synchronization. Phys. Rev. E **71**, 037203 (2005)
53. Huang, D.B.: Adaptive-feedback control algorithm. Phys. Rev. E **73**, 066204 (2006)
54. Chen, M., Zhou, D.: Synchronization in uncertain complex networks. Chaos **16**, 013101 (2006)
55. Vincent, U.E., Guo, R.W.: Finite-time synchronization for a class of chaotic and hyperchaotic systems via adaptive feedback controller. Phys. Lett. A **375**, 2322–2326 (2011)
56. Guo, R.W.: Finite-time stabilization of a class of chaotic systems via adaptive control method. Commun. Nonlinear Sci. Numer. Simul. **17**, 255–262 (2012)
57. Li, R.H., Chen, W.S., Li, S.: Finite-time stabilization for hyper-chaotic Lorenz system families via adaptive control. Appl. Math. Model. **37**, 1966–1972 (2013)
58. Podlubny, I.: Fractional Differential Equations: An Introduction to Fractional Derivatives, Fractional Differential Equations, to Methods of Their Solution and Some of Their Applications. Academic Press, New York(1998)
59. Das, S.: Functional Fractional Calculus for System Identification and Controls. Springer, Berlin (2008)
60. Petráš, I.: Fractional-Order Nonlinear Systems: Modeling Analysis and Simulation. Higher Education Press, Beijing (2011)
61. Tavazoei, M.S., Haeri, M.: Chaotic attractors in incommensurate fractional order systems. Phys. D **237**, 2628–2637 (2008)
62. Deng, W.H., Li, C.P., Lü, J.H.: Stability analysis of linear fractional differential system with multiple time delays. Nonlinear Dyn. **48**, 409–416 (2007)
63. Norelys, A.-C., Manuel, A.D.-M., Javier, A.G.: Lyapunov functions for fractional order systems. Commun. Nonlinear Sci. Numer. Simul. **19**, 2951–2957 (2014)
64. Manuel, A.D.-M., Norelys, A.-C., Javier, A.G., Rafael, C.-L.: Using general quadratic Lyapunov functions to prove Lyapunov uniform stability for fractional order systems. Commun. Nonlinear Sci. Numer. Simul. **22**, 650–659 (2015)
65. Hu, J.B., Lu, G.P., Zhang, S.B., Zhao, L.D.: Lyapunov stability theorem about fractional system without and with delay. Commun. Nonlinear Sci. Numer. Simul. **20**, 905–913 (2015)
66. Hu, J.B., Zhao, L.D.: Stability theorem and control of fractional systems. Acta Phys. Sin. **62**, 240504 (2013)
67. Slotine, J.-J., Li, W.P.: Applied Nonlinear Control. Prentice Hall, New Jersey (1991)
68. Zhang, X.D.: Matrix Analysis and Applications. Tsinghua University Press, Beijing (2004)
69. Grigorenko, I., Grigorenko, E.: Chaotic dynamics of the fractional Lorenz system. Phys. Rev. Lett. **91**, 034101 (2003)
70. Odibat, Z.: A note on phase synchronization in coupled chaotic fractional order systems. Nonlinear Anal. **13**, 779–789 (2012)
71. Wu, X.J., Shen, S.L.: Chaos in the fractional-order Lorenz system. Int. J. Comput. Math **86**, 1274–1282 (2009)
72. Diethelm, K., Ford, N.J., Freed, A.D.: A predictor-corrector approach for the numerical solution of fractional differential equations. Nonlinear Dyn. **29**, 3–22 (2002)
73. Rössler, O.E.: An equation for continuous chaos. Phys. Lett. A **57**, 397–398 (1976)
74. Razminia, A., Majd, V.J., Baleanu, D.: Chaotic incommensurate fractional order Rössler system: active control and synchronization. Adv. Differ. Equ. **2011**, 15 (2011)
75. Yu, Y.G., Li, H.X., Su, Y.: The synchronization of three chaotic fractional-order Lorenz systems with bidirectional coupling. J. Phys. **96**, 012113 (2008)
76. Saeed, B., Ali, K.S., Mohammad, H.: Stabilization of fractional order systems using a finite number of state feedback laws. Nonlinear Dyn. **66**, 141–152 (2011)
77. Uğur, E.K., Ylmaz, U.: Controlling Rucklidge chaotic system with a single controller using linear feedback and passive control methods. Nonlinear Dyn. **75**, 63–72 (2014)